Limited atmospheric iron availability increase during the Pleistocene-Holocene transition in the Northern Hemisphere

SUPPLEMENTARY MATERIAL

François Burgay[1,2], Haley Derrod[2], Tobias Erhardt[3,4], Federico Scoto[2,5], Delia Segato[6,2], Niccolò Maffezzoli[2,5,7], Federico Dallo[5], Daniele Zannoni[2], Azzurra Spagnesi[2], Helle-Astrid Kjær[8], Hubertus Fischer[3], Cristiano Varin[2], Carlo Barbante[2,3], Andrea Spolaor[2,3,*]

[1] Department of Environmental Sciences, University of Basel, Basel, Switzerland

[2] Department of Environmental Sciences, Informatics and Statistics, Ca' Foscari University of Venice, Venice Mestre, Italy

[3] Climate and Environmental Physics, Physics Institute & Oeschger Centre for Climate Change Research, University of Bern, Bern, Switzerland

[4] Institute of Geosciences, Goethe University Frankfurt, Frankfurt am Main, Germany

[5] Institute of Polar Sciences, National Research Council, Venice Mestre, Italy

[6] European Commission, Joint Research Centre, Ispra, Italy

[7] Department of Earth System Science, University of California, Irvine, Irvine, United States of America

[8] Physics for Ice, Climate and Earth, Niels Bohr Institute, University of Copenhagen, Copenhagen, Denmark

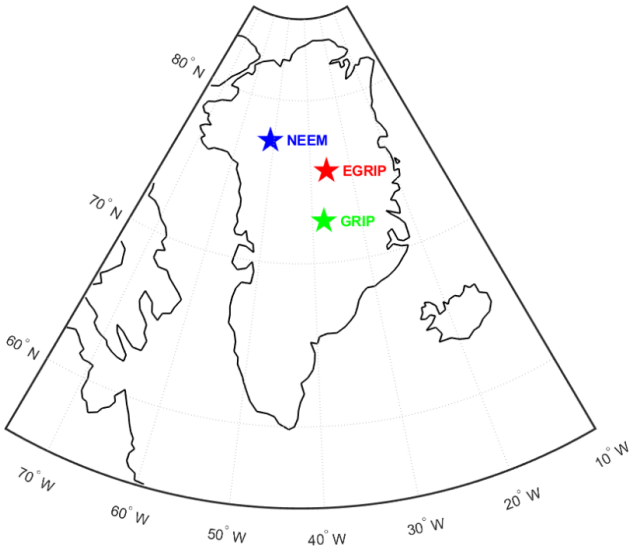

Figure S1 – Map of Greenland and location of three different Greenland ice-core locations discussed in the main text: EGRIP (red star), NEEM (blue star) and GRIP (green star).

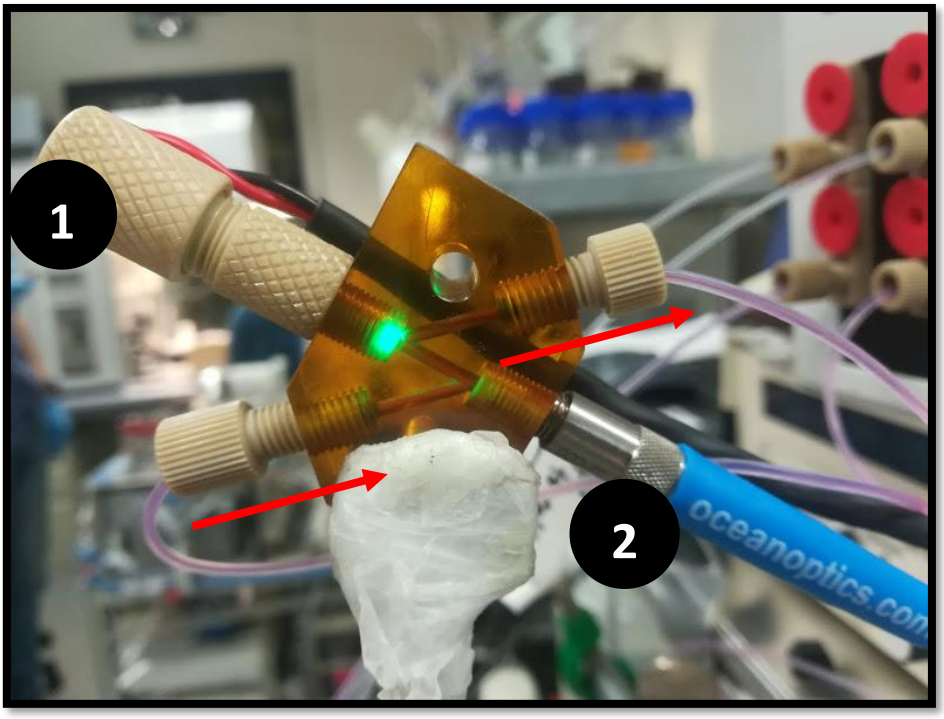

Figure S2– The Z cell used for DFe absorbance determination. The optical path is 1 cm. The upward inclination of the cell resulted to be beneficial to allow air bubbles to easily escape from the flow cell. Red arrows refer to the direction of the flow. 1) LED at 525 nm, 2) the fiber optics connected to the spectrophotometer. The transmittance signal was collected every second and subsequently converted to absorbance value using the Lambert-Beer law.

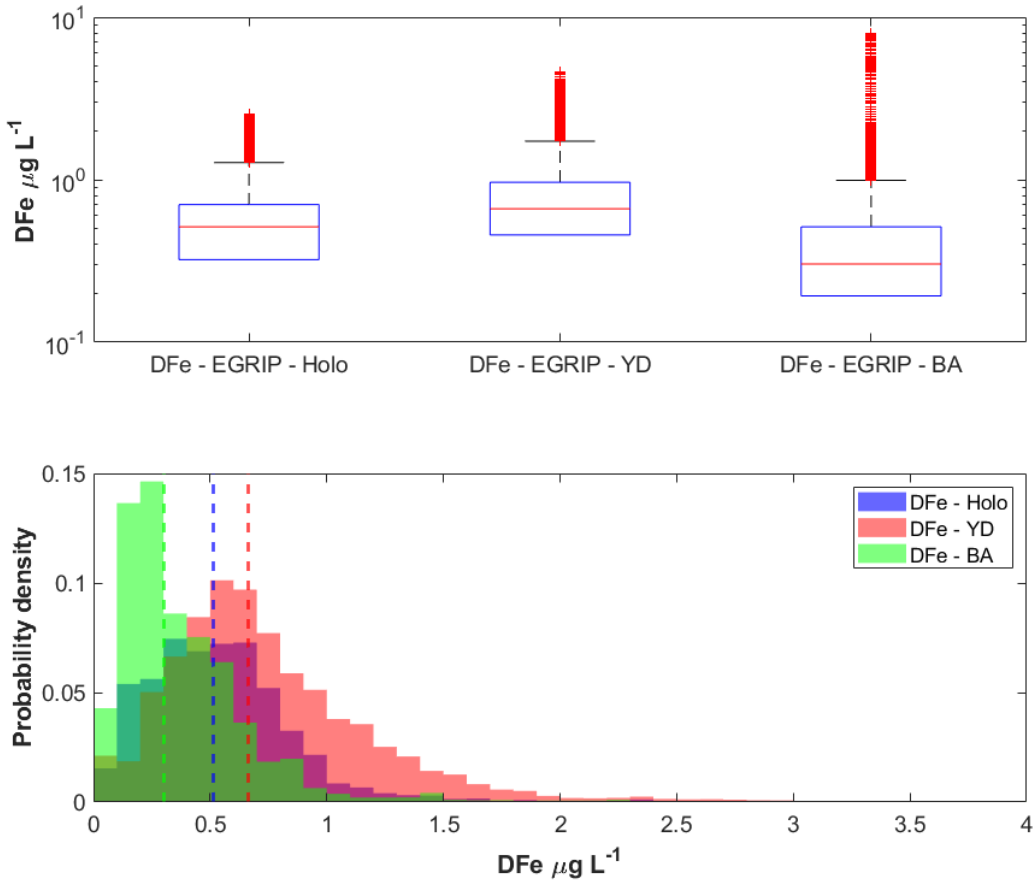

Figure S3 - Distribution of DFe during the Holocene (Holo), Younger Dyras (YD) and Bølling-Allerød (BA), when excluding volcanic eruptions. Upper panel: boxplot. Bottom panel: probability density distribution for DFe during Holocene (blue bars), YD (red bars) and BA (green bars). Dashed vertical lines refer to DFe median concentrations (blue, DFe – Holo, 0.51 µg L^{-1}; red, DFe – YD, 0.66 µg L^{-1}; green, DFe –BA, 0.30).

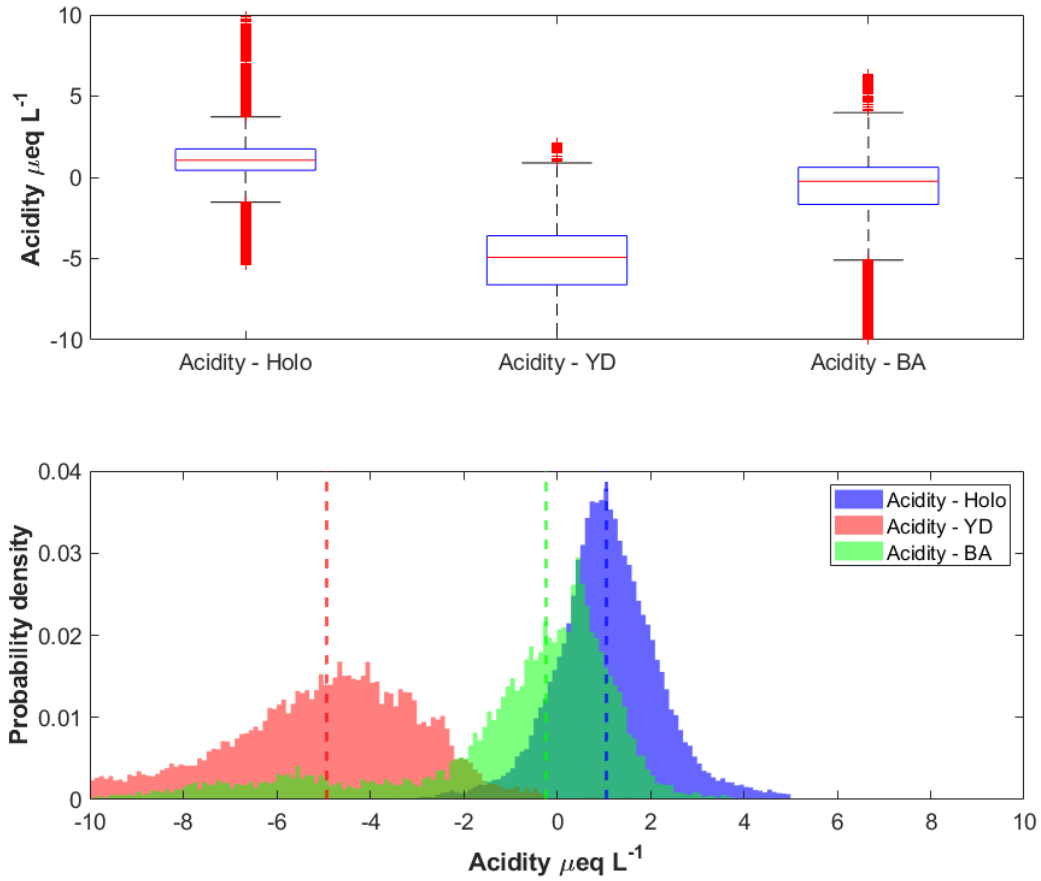

Figure S4 – Upper panel: Boxplot for acidity during the Early Holocene (left), YD (middle) and BA (right), when excluding volcanic eruptions. Bottom panel: probability density distribution for acidity during Early Holocene (blue bars), YD (red bars) and BA (green). Dashed vertical lines refer to acidity median values (blue, acidity – Holo, 1.06 µeq L^{-1}; red, acidity – YD, -4.93 µeq L^{-1}; green, acidity – BA, -0.24 µeq L^{-1}).

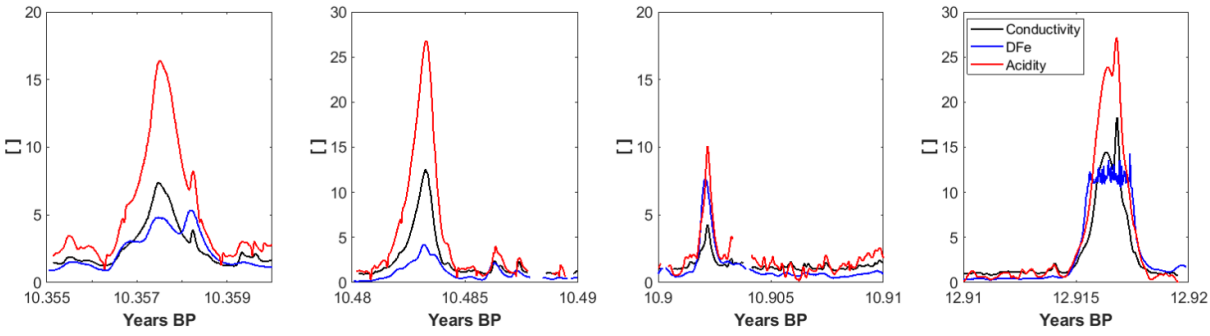

Figure S5 – Selected volcanic eruptions observed in the EGRIP ice core. Comparison between conductivity (black), DFe (blue) and acidity (red) for four selected volcanic eruptions. The cut peak for DFe in the right panel is due to the oversaturation of the detector. [ ] refers to µg L^{-1} for DFe, µS cm^{-1} for conductivity, and µeq L^{-1} for acidity. Other volcanic eruptions are shown in Table S2.

Table S1 – Concentration ranges for DFe calibration curves. STD = external standard prepared in ultrapure water.

Age /ka	Depth /m	Bag #	STD 1 /µg L^{-1}	STD 2 /µg L^{-1}	STD 3 /µg L^{-1}	STD 4 /µg L^{-1}
10.32-10.39	1150.60-1154.45	2093-2100	0.5	1	1.5	-
10.46-10.51	1159-95-1163.25	2110-2116	0.5	1	1.5	-
10.87-10.93	1190.20-1194.05	2165-2172	0.5	1	1.5	-
11.68-11.80	1243.00-1246.85	2261-2268	1	5	10	-
12.06-12.16	1256.20-1259.50	2285-2290	0.5	1	1.5	-
12.25-12.38	1262.80-1266.65	2297-2304	1	2.5	5	10
12.52-12.65	1271.60-1275.45	2313-2320	1	2.5	5	10
12.90-13.07	1284.80-1293.05	2337-2352	0.5	1	1.5	2.5

Table S2 – Identified volcanic eruptions in the analyzed EGRIP ice-core sections are reported with average SO_4^{2-} deposition in Greenland [*Lin et al.*, 2022], acidity, conductivity, DFe, Fe_{ICP} and DFe/FeICP. *n.a.* = not available, due to lack of data in the time series. Average DFe/FeICP were 0.40 during the Holocene, 0.02 during YD and 0.08 during BA. Highlighted eruptions (in bold) are shown in Figure S5.

Age	SO_4^{2-} deposition kg km^{-2} yr^{-1}	Acidity µeq L^{-1}	Conductivity µS cm^{-1}	DFe µg L^{-1}	Fe_{ICP} µg L^{-1}	DFe/Fe_{ICP}
10 345	111.0	*n.a.*	*n.a.*	> 12.0	68.8	> 0.18
10 357	**147.3**	**16.8**	**8.3**	**5.3**	**10.4**	**0.51**
10 480	**170.6**	**26.5**	**13.4**	**4.2**	**6.8**	**0.62**
10 900	**33.8**	**10.2**	**5.2**	**6.0**	**6.3**	**0.95**
11 705	96.9	0.6	5.1	6.0	60	0.10
12 600	226.0	2.7	6.9	22.2	*n.a.*	*n.a.*
12 917	**248.1**	**27.0**	**18.0**	**14.3**	**64.0**	**0.22**
12 959	n.a	4.3	3.1	3.7	12.3	0.30
12 994	47.4	6.3	3.2	9.5	10.0	0.90
13 027	272.8	27.4	18.5	17.2	66.2	0.26

SM Section 1. Processing of raw data from transmittance to concentration values

Here, we present an example on how data were treated from the raw transmittance values to sensitivity and blank corrected concentration values. Other details are reported in the main text.

1. **Processing of calibration files:** calibration files were obtained. In this example, CALIB49 and CALIB50 are the calibrations performed before and after the sample run that included EGRIP bag#2093 to EGRIP bag#2100. MQ, STD1, STD2 and STD3 refer to ultrapure water, first standard at 0.5 ng g^{-1} (or ppb), second standard at 1 ng g^{-1} and third standard at 1.5 ng g^{-1}, respectively. The intensities for every standards were selected when the signal was stable for at least 90 seconds. Gray vertical lines correspond to the breakpoints that segment the calibration measurements, red vertical lines correspond to the recorded times in the logbook where a standard was determined to be stable and shaded boxes indicate the windows which were determined to have the lowest variance, which will give the average transmittance value for each standard that was measured.

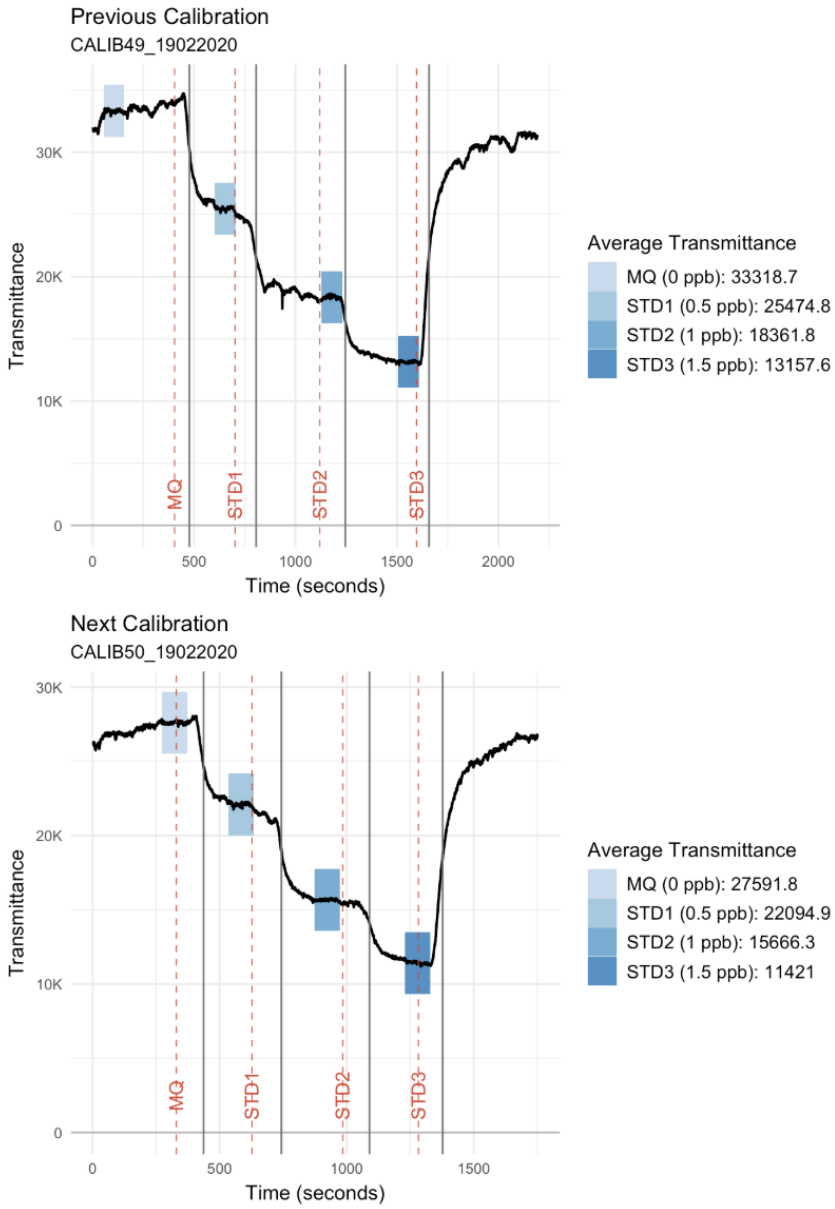

2. **Calibration signals were converted into absorbance values** following the Lambert-Beer equation.

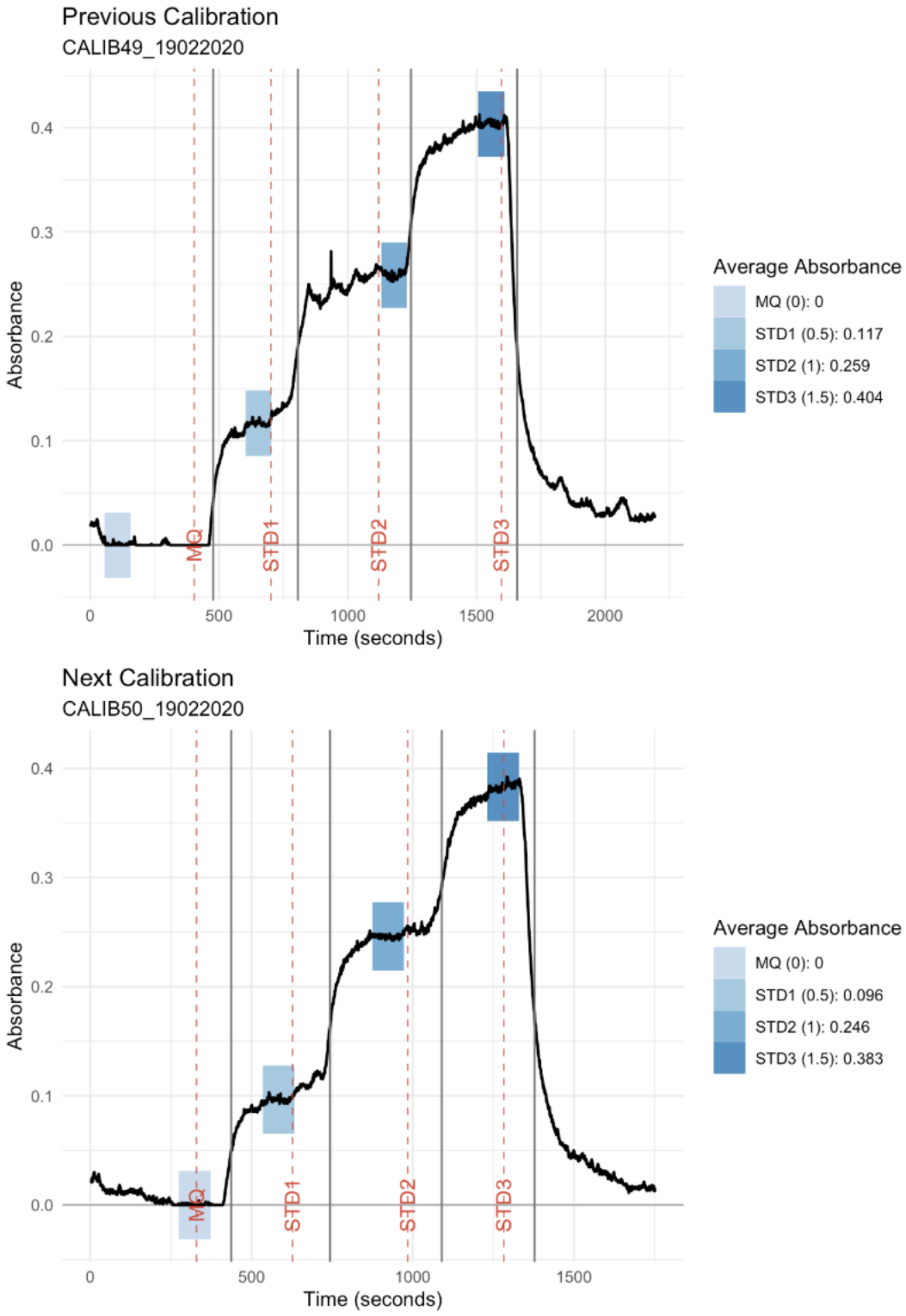

3. **Absorbance values are plotted against standard concentration to calculate the sensitivity for both curves.** Sensitivity values (i.e., the slope of the calibration curve) are fundamental for later correcting the data for instrumental sensitivity drift.

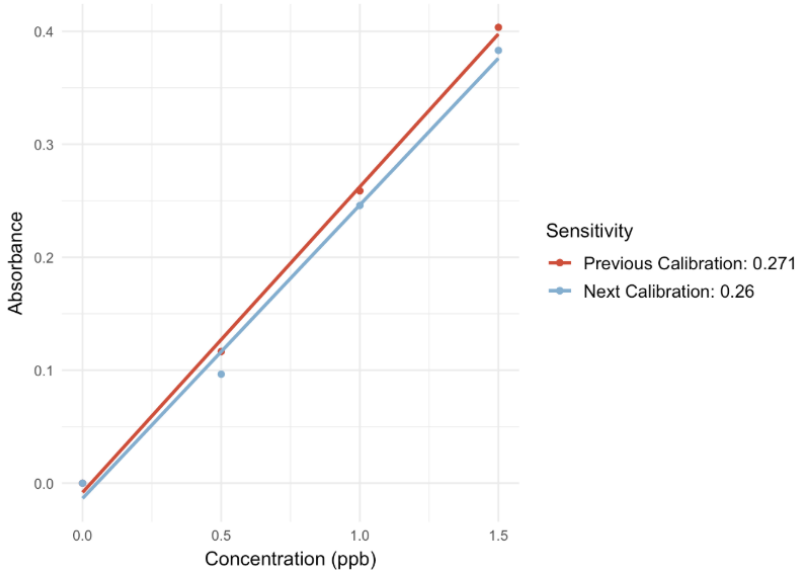

Previous calibration:

Sensitivity: 0.271

R^2 = 0.996

Next calibration:

Sensitivity = 0.260

R^2 = 0.989

Δ sensitivity = -4.1%

4. **Finding pre- (light blue rectangle) and post-sample (dark blue rectangle) baselines**

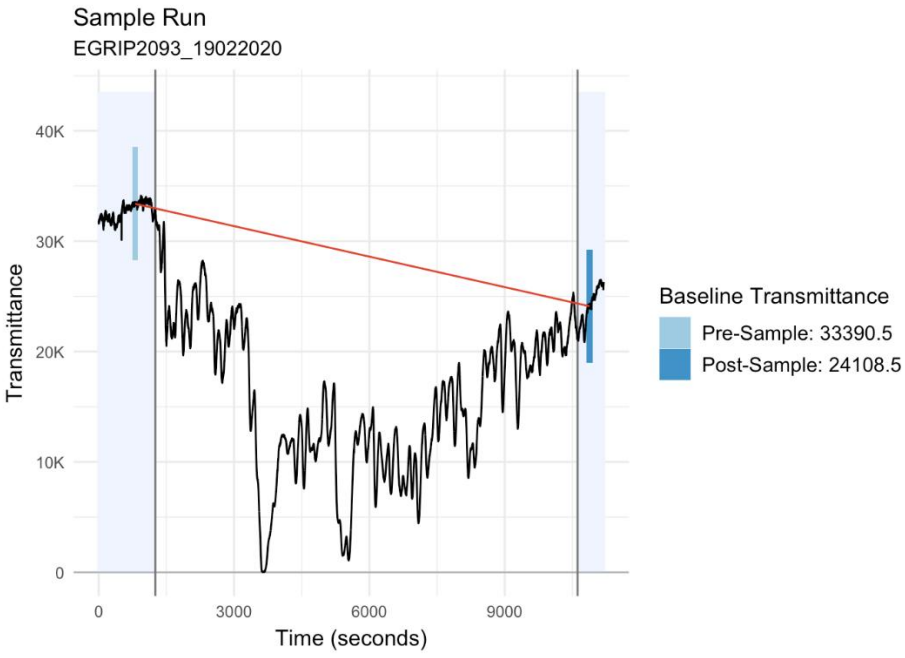

5. **Calculating the theoretical blank value at each time step of the sample run** to calculate the corresponding I0 in the Lambert-Beer law. We assumed a linear drift.

6. **Converting transmittance values into absorbance values** considering the blank drift.

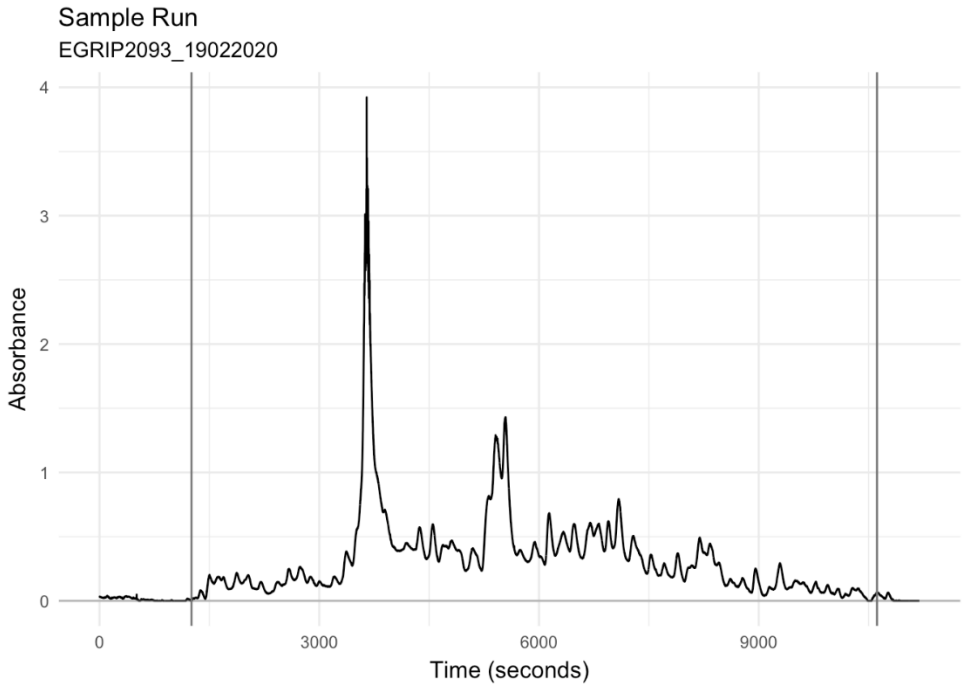

7. **Converting the absorbance signal into concentration values** (ppb), including the sensitivity correction (we assumed a linear sensitivity drift during the run).

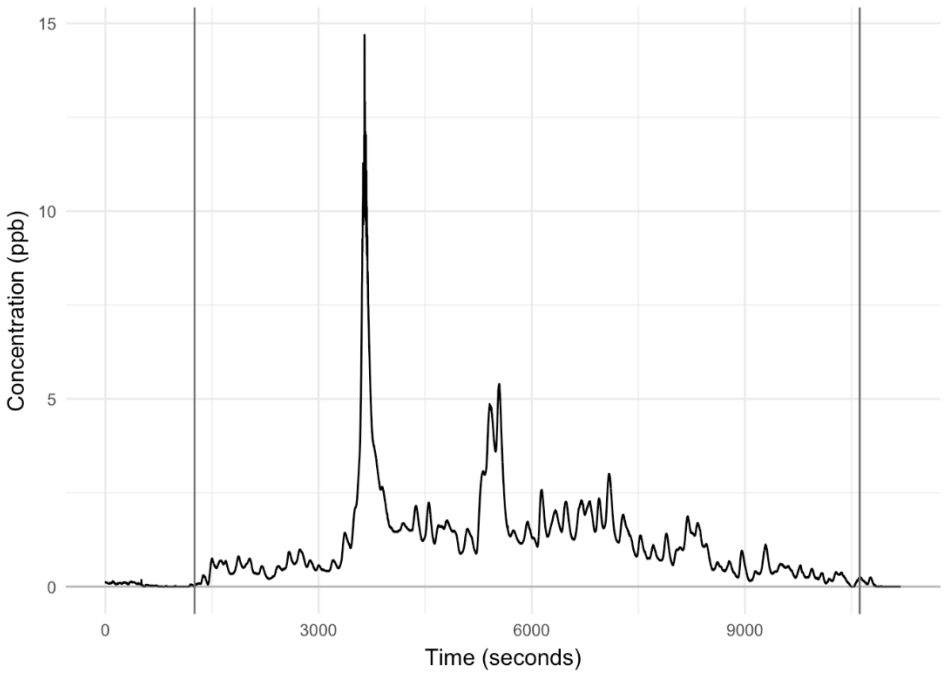

SM Section 2. DFe alignment with Bern CFA data

1. Corrected DFe and conductivity profiles are plotted against analysis time and a cross-correlation is performed between the two time series to find the time lag, i.e., where the ICCF has its highest values. The optimal time lag was found after 114 seconds. In this case the example refers to EGRIP bags #2110-2116.

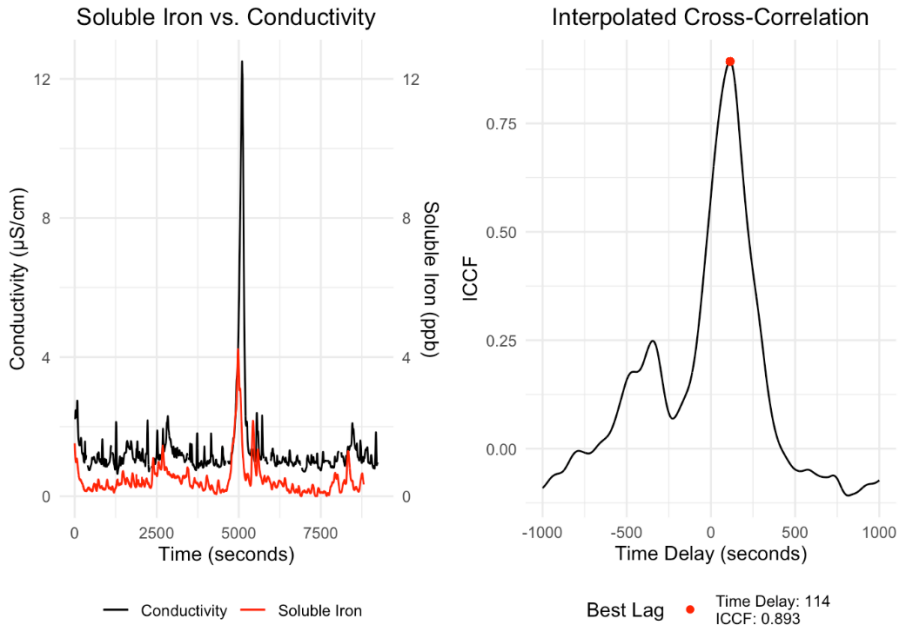

2. Corrected DFe and conductivity profiles are plotted against each other.

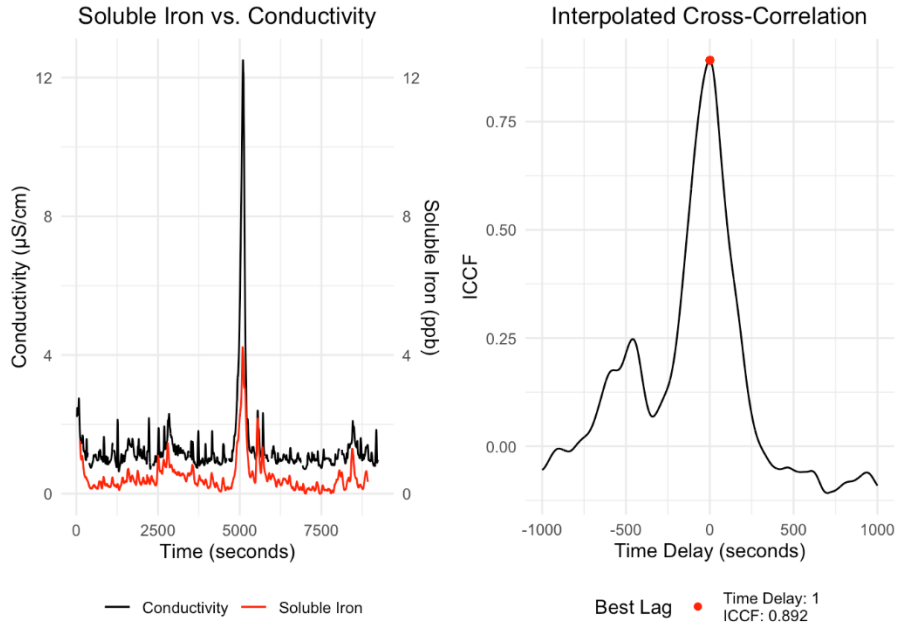

3. Once aligned, corrected DFe were plotted against depth following the available age scale and all the other available data from the Bern CFA (acidity, conductivity, dust and total iron).

SM Section 3. DFe, Fe_{ICP}, acidity and conductivity continuous profiles for the eight selected periods.

The following plots refer to the continuous temporal profile of the selected periods from the Early Holocene to the Bølling-Allerød.

1. Early Holocene runs

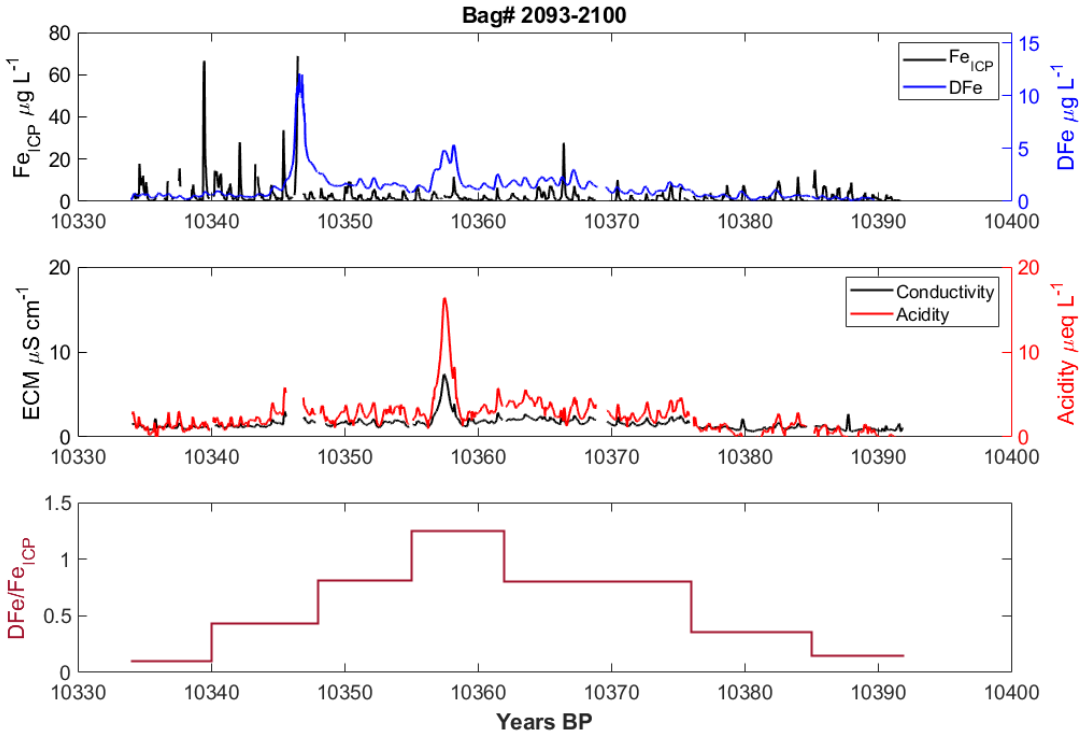

Bag #2096 shows DFe/Fe_{ICP} ratio values higher than 1. We attribute that to the relatively high DFe concentrations during that period, promoted by higher acidity values, which, due to some memory effect associated with the long mixing coils of the DFe line (> 2 meters).

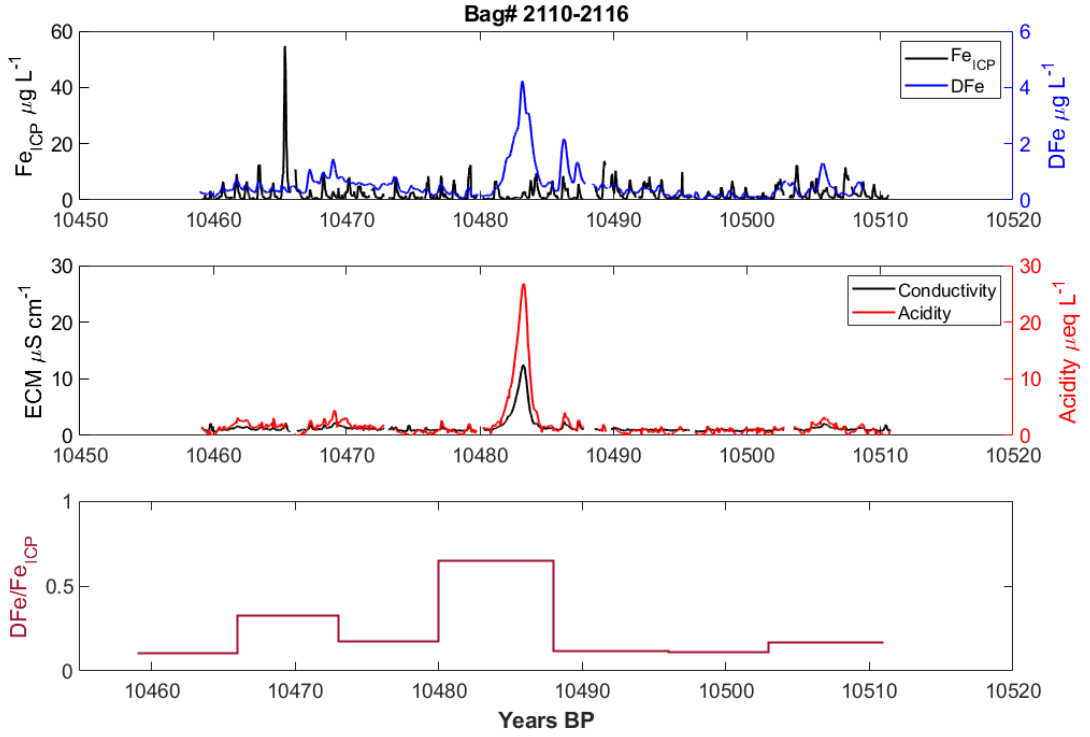
Bag# 2110-2116
Fe_ICP μg L-1
DFe μg L-1
Fe_ICP
DFe
ECM μS cm-1
Acidity μeq L-1
Conductivity
Acidity
DFe/Fe_ICP
Years BP

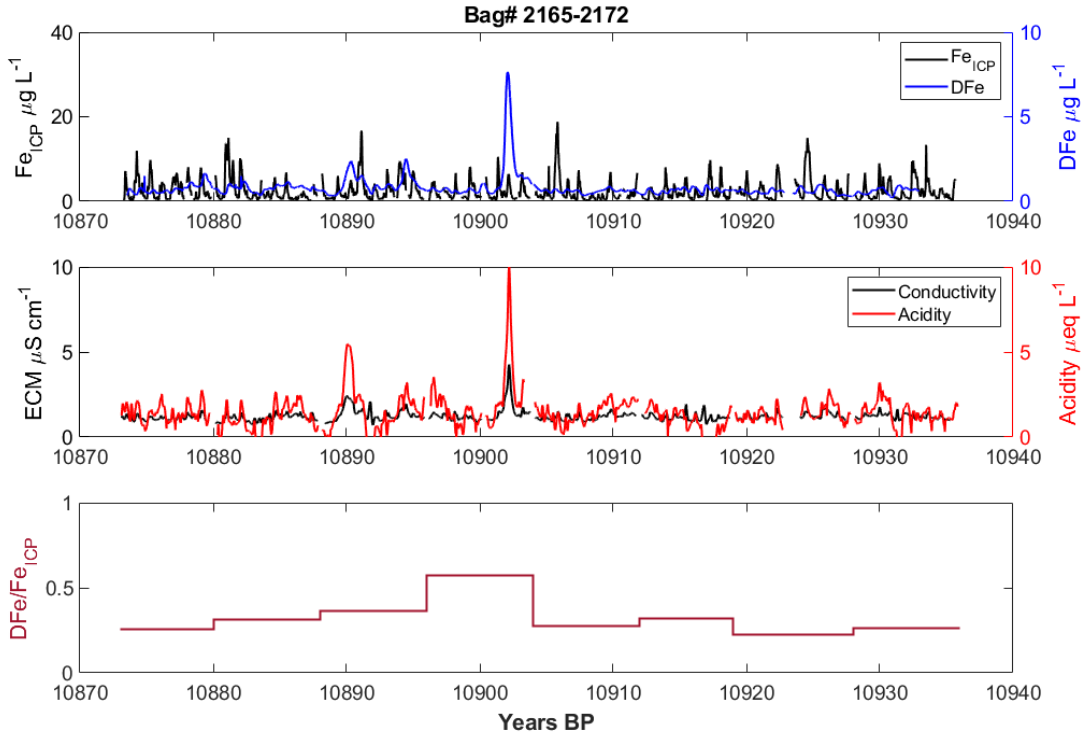
Bag# 2165-2172
Fe_ICP μg L-1
DFe μg L-1
Fe_ICP
DFe
ECM μS cm-1
Acidity μeq L-1
Conductivity
Acidity
DFe/Fe_ICP
Years BP

2. Younger Dryas *(including transition, bag#2261-2268)*

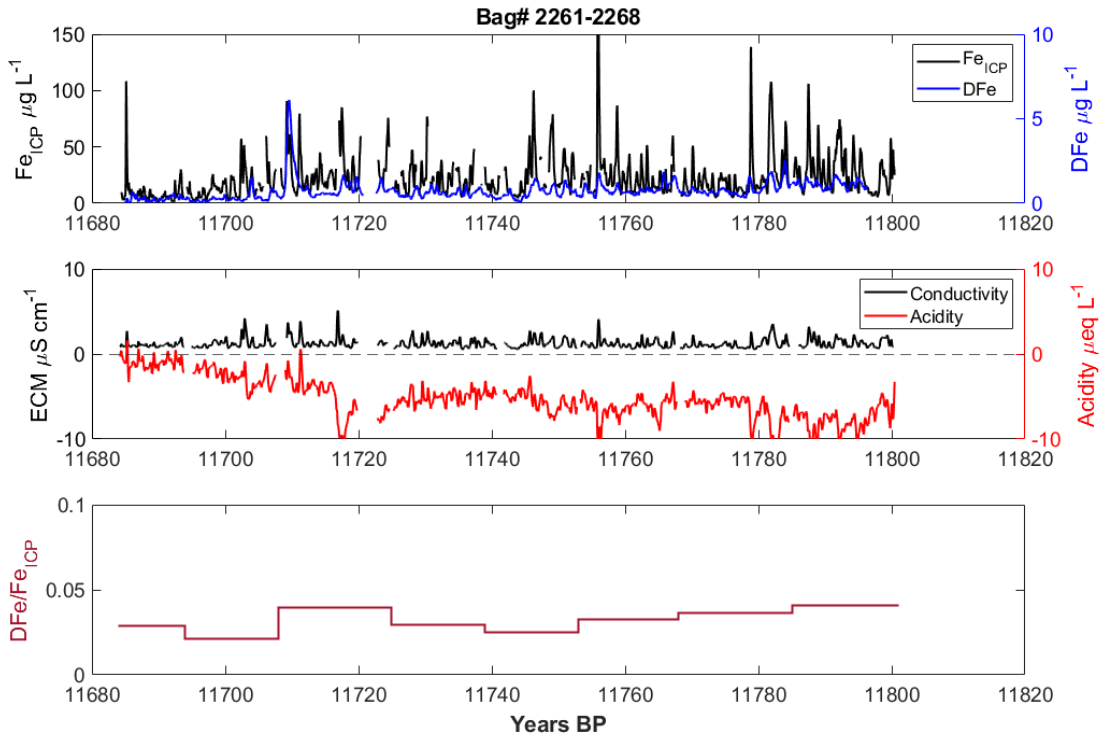

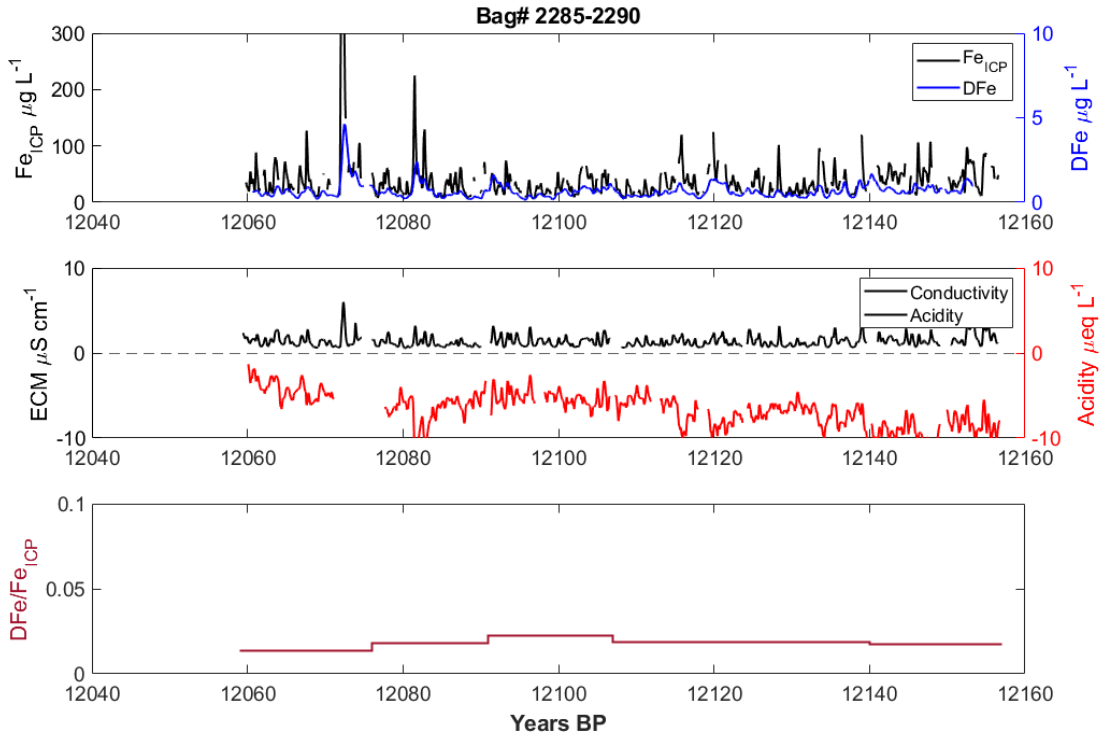

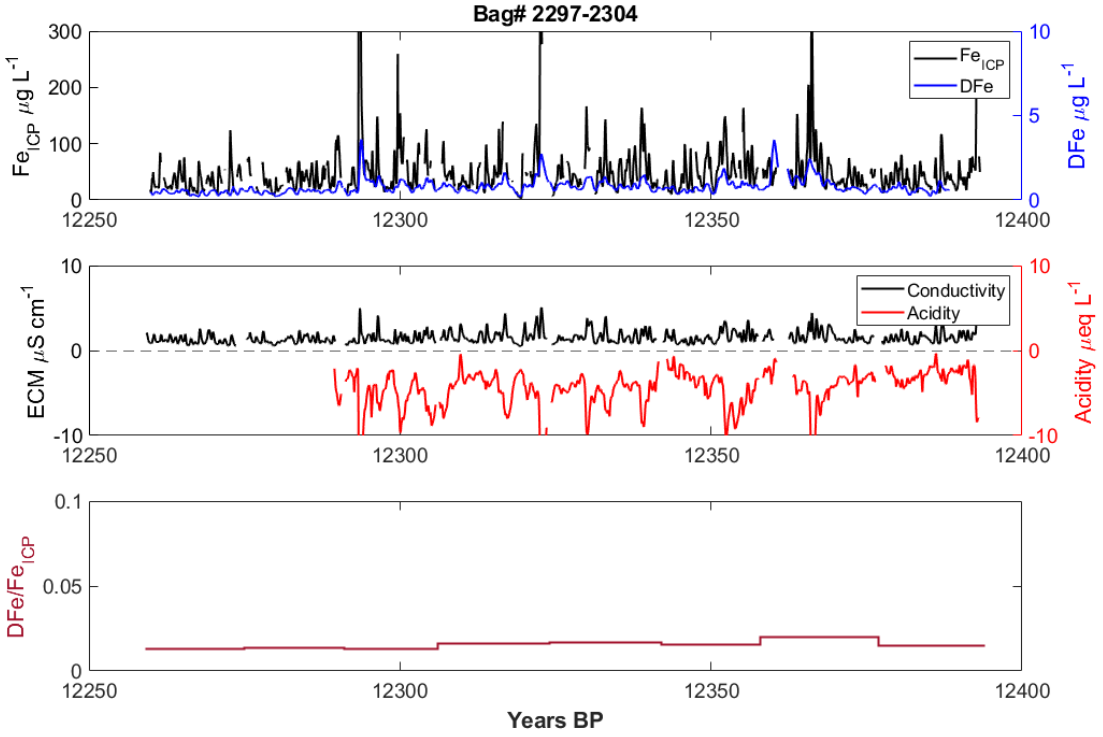
Bag# 2297-2304
Fe_ICP μg L-1
DFe μg L-1
Fe_ICP
DFe
ECM μS cm-1
Acidity μeq L-1
Conductivity
Acidity
DFe/Fe_ICP
Years BP

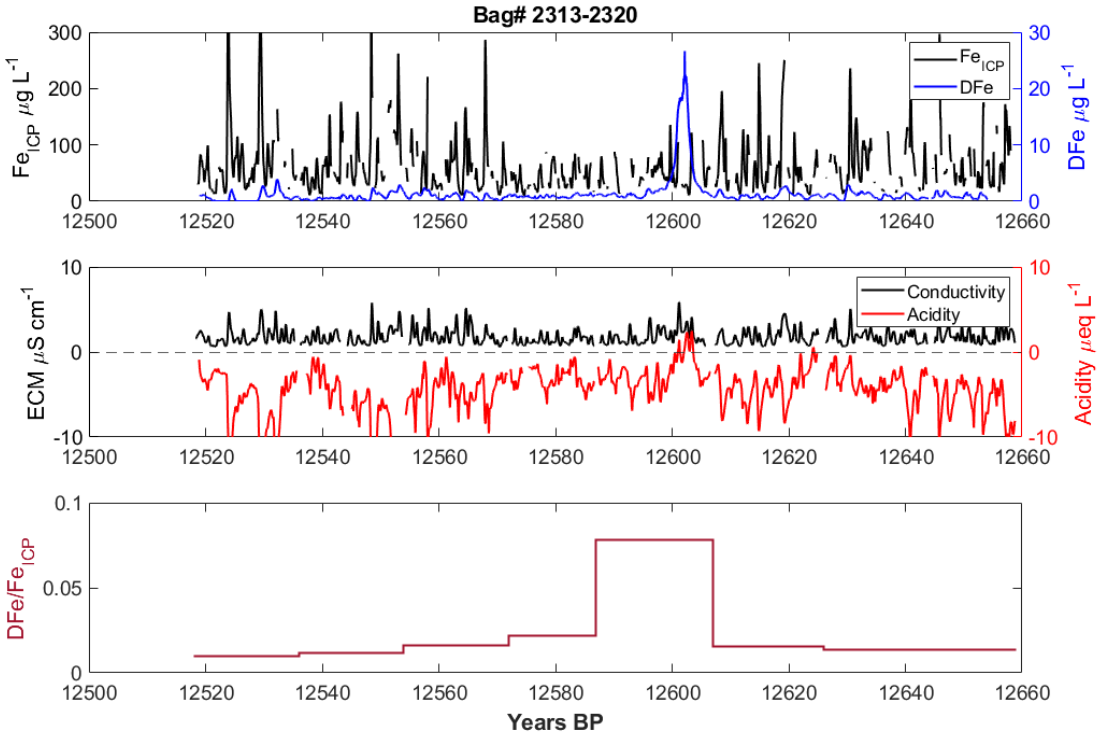
Bag# 2313-2320
Fe_ICP μg L-1
DFe μg L-1
Fe_ICP
DFe
ECM μS cm-1
Acidity μeq L-1
Conductivity
Acidity
DFe/Fe_ICP
Years BP

3. Bølling-Allerød

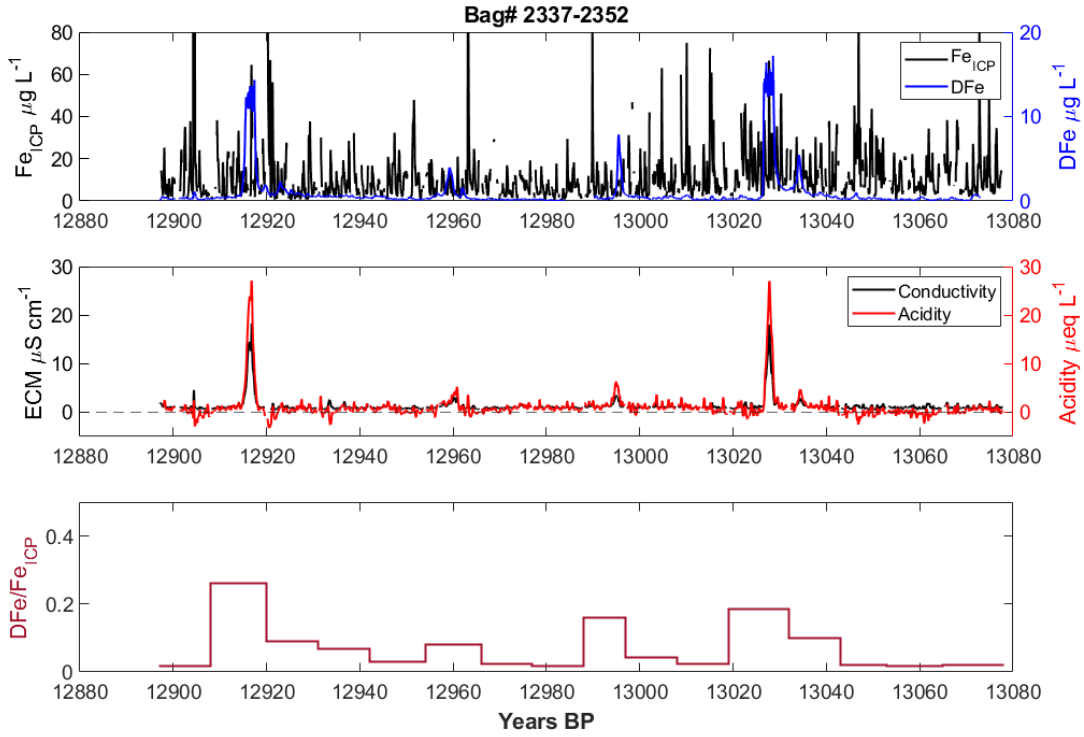

REFERENCES

Lin, J., A. Svensson, C. S. Hvidberg, J. Lohmann, S. Kristiansen, D. Dahl-Jensen, J. P. Steffensen, S. O. Rasmussen, E. Cook, and H. A. Kjær (2022), Magnitude, frequency and climate forcing of global volcanism during the last glacial period as seen in Greenland and Antarctic ice cores (60–9 ka), *Climate of the Past*, *18*(3), 485–506.